Article

Optical Activity Induced by Helical Arrangements of Tryptamine and 4-Chlorobenzoic Acid in Their Cocrystal

Hideko Koshima, Masaki Nagano, and Toru Asahi

J. Am. Chem. Soc., **2005**, 127 (8), 2455-2463• DOI: 10.1021/ja044472f • Publication Date (Web): 03 February 2005

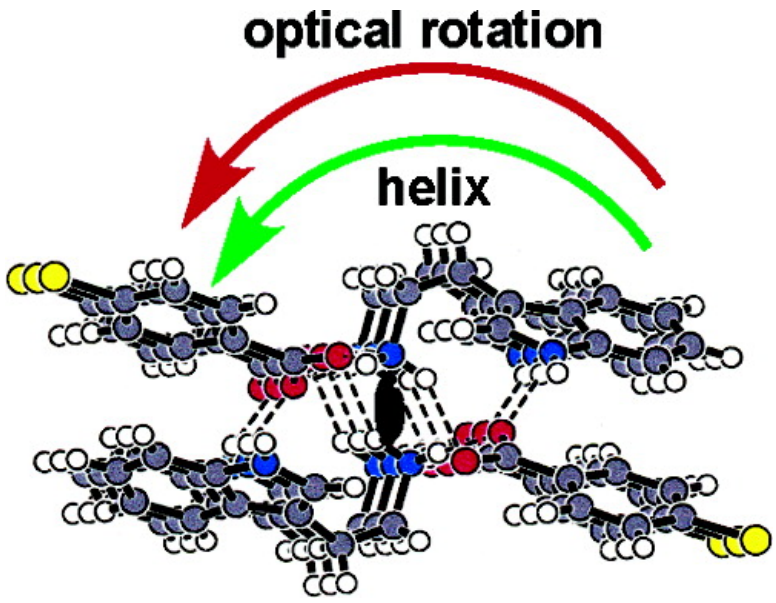

More About This Article

Additional resources and features associated with this article are available within the HTML version:

- Supporting Information
- Links to the 3 articles that cite this article, as of the time of this article download
- Access to high resolution figures
- Links to articles and content related to this article
- Copyright permission to reproduce figures and/or text from this article

View the Full Text HTML

J|A|C|S
ARTICLES
Published on Web 02/03/2005

Optical Activity Induced by Helical Arrangements of Tryptamine and 4-Chlorobenzoic Acid in Their Cocrystal

Hideko Koshima,*,† Masaki Nagano,† and Toru Asahi‡

Contribution from the Department of Applied Chemistry, Faculty of Engineering, Ehime University, Matsuyama 790-8577, Japan, and Major in Nano-Science and Nano-Engineering, Waseda University, Waseda, Shinjuku-ku, Tokyo 154-0012, Japan

Received September 13, 2004; E-mail: koshima@eng.ehime-u.ac.jp

Abstract: Optical rotatory powers of chiral cocrystals formed from the achiral molecules tryptamine and 4-chlorobenzoic acid were determined by the HAUP (high accuracy universal polarimeter) method. These cocrystals belonged to space group $P2_12_12_1$, and their absolute configuration was confirmed by the Flack parameter. In the *M*-crystal, 2-fold helical arrangements are formed in a counterclockwise direction between the two components through the quaternary ammonium salt bridge, hydrogen bond, and the aromatic $\pi-\pi$ interaction along the *c* axis, while clockwise helices alone exist in the *P*-crystal. Large rotatory powers $\rho_3^M = -355$ and $\rho_3^P = +352$ deg mm^{-1} were obtained along the *c* axis in the *M*- and *P*-crystal, respectively, at 632.8 nm and 303 K. The magnitude was 10 to 100 times larger than those for ordinary organic crystals. Further, it was confirmed that the negative sign was induced by the counterclockwise helical structures and the positive sign by the clockwise helices. In contrast, the rotations along the *a* and *b* axis which are in perpendicular directions to the screw axis were $\rho_1^M = +138$, $\rho_1^P = -140$ deg mm^{-1}, and $\rho_2^M = -56$, $\rho_2^P = +58$ deg mm^{-1}, much smaller than ρ_3^M and ρ_3^P . The results revealed that the helically arranged aromatic π electrons as well as the helical ionic and hydrogen bond networks in the crystal contributed to the enhancement of the magnitude of these rotations.

Introduction

Every chiral organic crystal has inherent optical activity.[1] The sign and the magnitude of the optical activity of an organic crystal should reflect the molecular structure as well as the packing arrangement because the freedom of molecules is severely restricted in the crystal lattice, which is very different from the high mobility of molecules in solution. However, the optical activity of organic crystals has been scarcely measured and therefore never correlated with the crystal structure until the present time. The reason for this is that the measurement of optical activity of a crystal is accompanied with much difficulty due to birefringence being 10^3 times larger birefringence than the gyration tensor, so in this case the latter effect is masked. The Kobayashi group successfully overcame the problems by use of the HAUP (high accuracy universal polarimeter) method.[2−4] The outline of the HAUP method is explained in the Results. However, the principle of the technique is to measure the intensity of light passing through a polarizer, followed by the crystal sample, and then by an analyzer. By measuring the intensity of the emergent light transmitted through the system as the azimuth angles of the polarizer are altered, it is possible to solve the optical equations governing the intensity and thus separate out the gyration tensor and birefringence. Furthermore, in the HAUP method, systematic errors originating in the parasitic ellipticities of the polarizer and analyzer are removed by using an optically inactive crystal.

We have prepared several series of chiral cocrystals from two different achiral molecules by self-assembly.[5,6] Such chiral cocrystals are useful as starting materials for absolute asymmetric synthesis by solid-state reaction[7] as well as nonlinear optical materials.[8] Furthermore, this type of chiral crystallization is relevant to the prebiotic origin of chirality.[9] These materials include helical-type cocrystals of tryptamine with various carboxylic acids[10] and phenanthridine with 3-indolepropionic acid.[11] The crystal chirality is generated from helical packing

† Ehime University.
‡ Waseda University.

(1) Lowry T. M. *Optical Rotatory Power*; Dover Publications: New York, 1964.
(2) Kobayashi, J.; Uesu, Y. *Appl. Crystallogr.* **1883**, *16*, 204−211.
(3) Kobayashi, J.; Kumomi, H.; Saito, K. *J. Appl. Crystallogr.* **1986**, *19*, 377−381.
(4) Kobayashi, J.; Asahi, T.; Takahashi, S.; Glazer, A. M. *J. Appl. Crystallogr.* **1988**, *21*, 479−484.
(5) (a) Koshima, H.; Matsuura, T. *J. Synth. Org. Chem.* **1998**, *56*, 268−279 (Japanese). (b) Koshima, H.; Matsuura, T. *J. Synth. Org. Chem.* **1998**, *56*, 466−477 (Japanese).
(6) Koshima, H. In *Organic Solid State Reactions*; Toda, F., Ed.; Kluwer Academic Publishers: Dordrecht, 2002; pp 189−268.
(7) (a) Koshima, H.; Ding, K.; Chisaka, Y.; Matsuura, T. *J. Am. Chem. Soc.* **1996**, *118*, 12059−12065. (b) Koshima, H.; Nakagawa, T.; Matsuura, T.; Miyamoto, H.; Toda, F. *J. Org. Chem.* **1997**, *62*, 6322−6325.
(8) (a) Koshima, H.; Hamada, M.; Yagi, I.; Uosaki, K. *Cryst. Growth Des.* **2001**, *1*, 467−471. (b) Koshima, H.; Miyamoto, H.; Yagi, I.; Uosaki, K. *Cryst. Growth Des.* **2004**, *4*, 807−811.
(9) Addadi, L.; Lahav, M. In *Origin of Optical Activity in Nature*; Waker, D. C., Ed.; Elsevier: New York, 1979: Chapter 14.
(10) (a) Koshima, H.; Khan, S. I.; Garcia-Garibay, M. A. *Tetrahedron: Asymmetry* **1998**, *9*, 1851−1854. (b) Koshima, H.; Honke, S. *J. Org. Chem.* **1999**, *64*, 790−793. (c) Koshima, H.; Honke, S.; Fujita, J. *J. Org. Chem.* **1999**, *64*, 3916−3921. (d) Koshima, H.; Honke, S.; Miyauchi, M. *Enantiomer* **2000**, *5*, 125−128. (e) Koshima, H.; Miyauchi, M.; Shiro, M. *Supramol. Chem.* **2001**, *13*, 137−142. (f) Koshima, H.; Miyauchi, M. *Cryst. Growth Des.* **2001**, *1*, 355−357.

arrangement in a unidirection between the two achiral molecules through intermolecular noncovalent bonds such as hydrogen bonds and $\pi-\pi$ interactions. As a matter of course, the cocrystals from achiral molecules are optically active, but this property is lost immediately when they are dissolved in solution. Hence, we would like to measure the optical activity in the crystalline state and correlate this with the helical structure.

The huge rotatory power ($\rho_3 = +9200$ deg mm^{-1}) of a helical polymer film poly(L-lactide) $-[-OCH(CH_3)CO-]_n-$ has been reported by the Kobayashi group, which is 2 or 3 orders of magnitude larger than those of ordinary crystals.[12] We were surprised at this large value and realized the significant contribution of the helical structure to the enhancement of optical activity. The rotatory powers of several chiral organic crystals, Rochelle salt,[13] sodium ammonium tartrate,[14] tartaric acid,[15] triglycine sulfuric acid,[16] L-glutamic acid,[17] L-aspartic acid,[18] lysozyme,[19] and D-mannitol[20] were also reported, but the quoted papers presented no discussion of the structure−rotation relationship. An earlier attempt of HAUP measurements of optical activity of chiral crystals from an achiral oxo amide did not determine the absolute configuration, and therefore the structure−rotation correlation was not discussed.[21] In the case of inorganic crystals, an anisotropic atomic polarizability theory of optical activity was proposed by Glazer and co-workers, namely that the sign and the magnitude of optical rotation could be calculated by using the maximum anisotropic polarizability components in a helix.[22,23] The agreement between theory and experiment was excellent for crystals such as α-quartz and α-$AlPO_4$. However, the application of this theory to tartaric acid crystals failed due to the strong hydrogen bond network formed in the lattice.[15] Recently, calculations of optical rotations of the isomorphous tetraphenylmethane crystals Ph_4X where X = C, Si, Ge, Sn, and Pb have been reported based on the dipole−dipole theory, but the experimental measurements were not carried out.[24] Thus, the atomic polarizability approach has its own limitations in application to ordinary organic crystals, in which noncovalent intermolecular interactions such as hydrogen bonds and $\pi-\pi$ interactions of aromatic moieties are predominant in the lattice.

Herein the rotatory powers of helical-type cocrystal formed between tryptamine and 4-chlorobenzoic acid[10e] were determined by the HAUP method. This is the first measurement of the optical activity of organic−organic cocrystal formed from two different achiral molecules. This cocrystal was selected from a series of helical-type cocrystals of tryptamine and carboxylic acids,[10] because millimeter size single crystals could be prepared. Although the HAUP method was theoretically established, the technical problem of sample polish has not yet been solved to attain optically smooth plane-parallel specimens. As pointed out by Folcia et al., the polish scratches that remained on the crystal surfaces led to an increase in the systematic errors.[25] In the measurement of deteriorative crystals, the surface problem was more serious. Kaminsky and Grazer have developed a new tilter method originally based on the HAUP technique, whereby it is possible to complete the scan quickly within several minutes.[26] Then a tartaric acid crystal, the surface of which deteriorates by humidity, is submitted to the tilter method to determine its rotatory powers.[15] In our present HAUP measurement, after much trial and error, we could overcome the sample polish problem by using soft Fe_2O_3 polish agent and obtain satisfactorily the rotatory powers of the cocrystal from tryptamine and 4-chlorobenzoic acid. The correlation of the large rotatory powers with the helical structures is discussed.

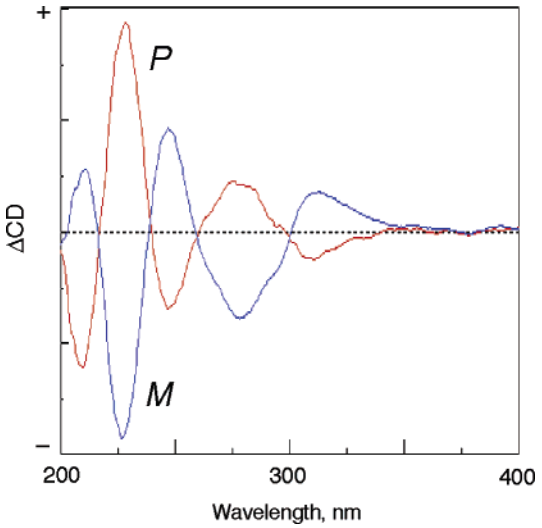

Figure 1. Solid-state CD spectra of powdered crystals of *M*- and *P*-**1·2** as Nujol mulls.

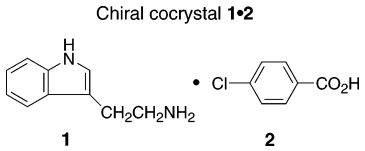

Results

Crystals and Optical Nature. The cocrystal **1·2** of tryptamine **1** and 4-chlorobenzoic acid **2** belonged to the orthorhombic, space group $P2_12_12_1$, and its cell constants were $a = 15.141(2)$ Å, $b = 16.700(4)$ Å, $c = 6.269(1)$ Å, $Z = 4$.[10e] The crystals were colorless and gave the high melting point of 203−204 °C due to their ionic character. Both enantiomorphous crystals were obtained by spontaneous crystallization from methanol solution and discriminated by the measurement of solid-state (powder) CD spectra as Nujol mulls (Figure 1). A grain of the single crystal was cut into two pieces. The absolute structure of the half crystal was determined to be *P*-**1·2** by the Flack parameter

(11) (a) Koshima, H.; Hayashi, E.; Matsuura, T.; Tanaka, K.; Toda, F.; Kato, M.; Kiguchi, M. *Tetrahedron Lett.* **1997**, *38*, 5009−5012. (b) Koshima, H.; Hayashi, E.; Matsuura, T. *Supramol. Chem.* **1999**, *11*, 57−66.
(12) Kobayashi, J.; Asahi, T.; Ichiki, M.; Oikawa, A.; Suzuki, H.; Watanabe, T.; Fukuda, E.; Shikinami, Y. *J. Appl. Phys.* **1995**, *77*, 2957−2973.
(13) Kobayashi, Z.; Uchino, K.; Asahi, T. *Phys. Rev.* **1991**, *B43*, 5706−5712.
(14) Lingard, R. J. 1994 *Dphil Thesis*, University of Oxford; see Kaminsky, W. *Rep. Prog. Phys.* **2000**, *63*, 1575−1640.
(15) Mucha, D.; Stadnicka, K.; Kaminsky, W.; Glazer, A. M. *J. Phys.: Condens. Matter* **1997**, 10829−10842.
(16) Kobayashi, Z.; Uchino, K.; Matsuyama, H.; Saito, K. *J. Appl. Phys.* **1991**, *69*, 409−413.
(17) Asahi, T.; Utsumi, H.; Itagaki, Y.; Kagomiya, I.; Kobayashi, Z. *Acta Crystallogr.* **1996**, *A52*, 766−769.
(18) Asahi, T.; Takahashi, M.; Kobayashi, Z. *Acta Crystallogr.* **1997**, *A53*, 763−771.
(19) Kobayashi, Z.; Asahi, T.; Sakurai, M.; Kagomiya, I.; Asai, H.; Asami, H. *Acta Crystallogr.* **1998**, *A54*, 581−590.
(20) Kaminsky, W.; Glazer, A. M. *Z. Krystallogr.* **1997**, *212*, 283−296.
(21) Asahi, T.; Nakamura, M.; Kobayashi, J.; Toda, F.; Miyamoto, H. *J. Am. Chem. Soc.* **1997**, *119*, 3665−3669.
(22) Glazer, A. M.; Stadnicka, K. *J. Appl. Crystallogr.* **1986**, *19*, 108−122.
(23) Devarajan, V.; Glazer, A. M. *Acta Crystallogr.* **1986**, *A42*, 560−569.
(24) Claborn, K.; Kahr, B.; Kaminsky, W. *CrystEngComm* **2002**, *4*, 252−256.
(25) Folcia, C. L.; Ortega, J.; Etxebarria, J. *J. Phys. D: Appl. Phys.* **1999**, *32*, 2266−2277.
(26) Kaminsky, W.; Glazer, A. M. *Ferroelectrics* **1996**, *183*, 133−141.

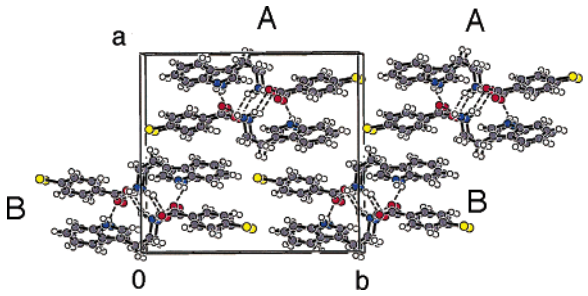

Figure 2. Helical molecular arrangements formed in *M*-**1**·**2** along *c* axis.

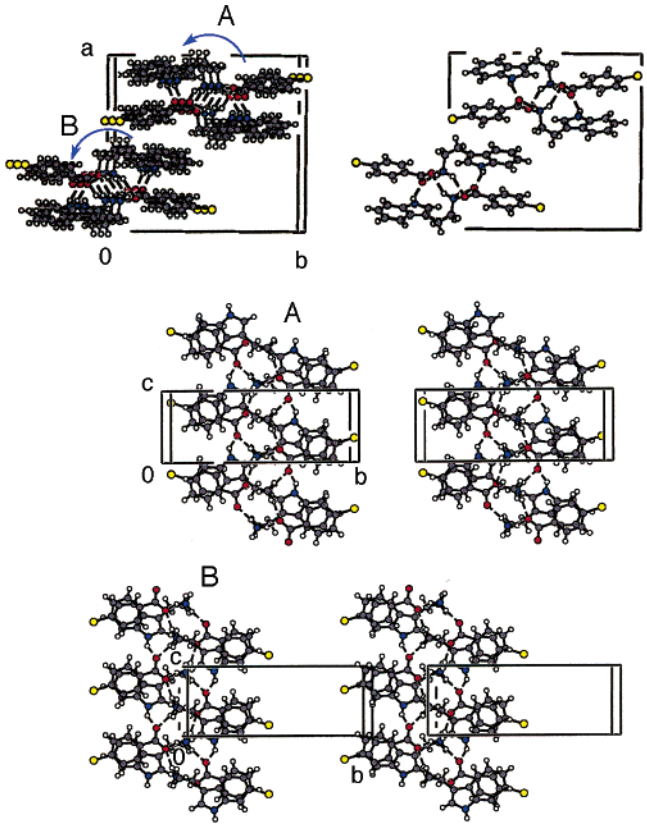

Figure 3. Stereoviews of helical arrangements in *M*-**1**·**2**.

$\chi = -0.02(4)$ based on the anomalous dispersion of the chlorine atom with Cu Kα radiation. The second half was submitted to solid-state CD spectral measurement as a Nujol mull to give the curve P in Figure 1. Thereafter, absolute structures of given single crystals could be determined by their solid-state CD spectra.

In the cocrystal, two kinds of 2-fold helical arrangements A and B are formed through the $NH_3^+\cdots{}^-O_2C$ quaternary ammonium salt bridges (1.79, 1.80, 2.11 Å) between the amino group of **1** and the carboxylic acid group of **2** along the *c* axis (Figure 2). Another In−NH···O−C hydrogen bond (1.96 Å) formed between the indole imino group of **1** and the carboxylic acid group of **2** plays a role in fixation of the helical structures. In both the A and B helices, the phenyl ring of **1** and the indole ring of **2** are arranged in an almost parallel manner with a small dihedral angle (2.6(1)°) and short plane-to-plane distances (3.42−3.66 Å). As understood from the stereoviews of *M*-crystal (Figure 3), the difference between the helices A and B is that the indole imino group of **1** of A is arranged upward along the *c* axis and oppositely downward in B. The direction of both A and B helical structures is counterclockwise. It is understandable that the crystal chirality is generated through the unidirectional helicity in the lattice.

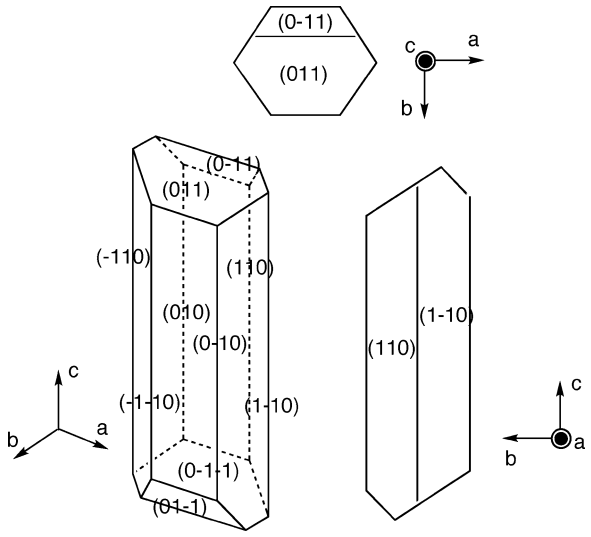

Figure 4. Crystal habit of *M*-**1**·**2**.

Single crystals of around 10-mm length were prepared for the HAUP measurement by slow evaporation or slow temperature decrease of methanol solutions of stoichiometric mixtures of both components. The crystal morphology was a six-sided rodlike habit (Figure 4). HAUP measurements of (100), (010), and (001) faces were necessary to clarify the gyro-optical properties of the crystal. The (010) face was grown, but the (100) and (001) faces were poorly developed.

To determine the signs of the gyration tensor components, it is necessary to clarify the optical nature of the specimen. Conoscopic pictures observed on the (010) plane are shown in Figure 5. From Figure 5a, it was clear that the *a* axis was optical *Y* axis, since it was perpendicular to the optical plane, (010) plane. Birefringence increased when the *c* axis paralleled the *Z*′ axis of the 1−6 wave plate as shown in Figure 5b, while the reverse was the case in Figure 5c. Therefore the *c* axis must be the optical *Z* axis. The order of refractive index is expressed to be $n_a < n_c < n_b$. Fast and slow components in the crystal could be determined.

Preparation of thin plane-parallel plate specimens is necessary for the HAUP measurement. Absolute structures were first confirmed piece by piece by the measurement of CD spectra using the portions of single crystals (Figure 1). The crystals were polished successively with 5, 1, and 0.3 μm Al_2O_3 lapping film. Moisture was introduced by breathing on the lapping film as a lubricating agent. However, the organic crystals were much softer than inorganic crystals, and therefore Al_2O_3 was too hard in removing small scratches and giving smooth optical surfaces for the HAUP measurement. Furthermore, three cleavage planes of (010), (110), and (−110), which reflect the weak intermolecular interaction as understood from the packing arrangement in Figure 2, made the polishing more difficult. After much trial and error, we could attain the smooth optical surfaces by using 0.3 μm Fe_2O_3 lapping film (which is much softer than Al_2O_3) and a polishing tool of $^1/_{10}$ weight at the last stage, leading to the HAUP measurements with satisfactorily small systematic errors and good reproducibility. The (100) and (001) specimens were very carefully prepared to be perpendicular to

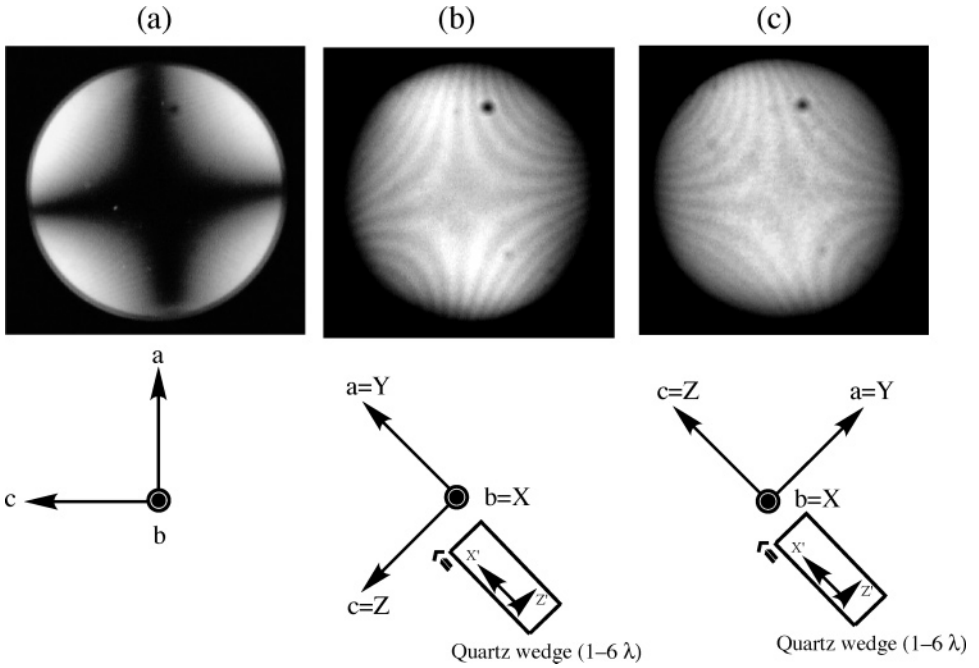

Figure 5. Conoscopic pictures observed on (010) plane of cocrystal **1·2**. (a) Figure at an extinction position; (b and c) figures at 90° different diagonal positions. λ, wavelength.

the (010) plane by observing with a microscope during the polish because the natural faces were poorly grown (Figure 4).

Gyro-optical Properties. The improved HAUP method[3] was adopted to determine all the components of gyration tensor g and birefringence Δn. The principle of the HAUP method is to measure the intensity of emergent light passing through a polarizer, crystal sample, and then by analyzer as azimuth angles of the polarizer and analyzer are independently altered. First, we would like to explain briefly the improved HAUP method expressed by the following relative intensity formulas $\Gamma(\theta', \mathrm{Y}', p, q)$.

$$\Gamma(\theta', \mathrm{Y}', p, q) = A(\theta', p, q) + B(\theta', p, q)\mathrm{Y}' + \mathrm{Y}'^2 \quad (1)$$

where

$$A(\theta', p, q) = A_0 + (\gamma - 2k)^2 \sin^2(\Delta/2) + (\gamma - 2k)\,\delta\mathrm{Y} \sin\Delta + (\delta\mathrm{Y})^2 \cos^2(\Delta/2) + 4 \sin^2(\Delta/2)\theta'^2 \quad (2)$$

and

$$B(\theta', p, q) = (\gamma - 2k) \sin\Delta + 2\delta\mathrm{Y} \cos^2(\Delta/2) + 4 \sin^2(\Delta/2)\theta' \quad (3)$$

Here Δ designates retardation, θ', the reading value of the azimuth of the incident light, and Y', the reading value of the deflecting angle of the analyzer from the crossed-Nicols condition. $\gamma = p - q$ is the systematic error derived from the parasitic ellipticities p and q of the polarizer and analyzer. $\delta\mathrm{Y}'$ is the systematic error of the deflecting angle of the analyzer from the crossed-Nicols position, k ellipticity of the eigen-polarization of light travelling in the crystal. We adopt the simple HAUP method[2] for the sake of brevity.

(i) Fix the relative position of the polarizer and analyzer at $\mathrm{Y}' = 0$ at and $\Gamma(\theta', 0, p, q) = A(\theta')$ is measured as a function of θ'. From the linear relation between $A(\theta')$ and θ'^2, $\sin^2(\Delta/2)$ can be obtained.

(ii) Fix θ' at zero, and $\Gamma(0, \mathrm{Y}', p, q)$ can be measured as a function of Y'. In this case, B(0), which is expressed by

$$B(0) = (\gamma - 2k) \sin\Delta + 2\delta\mathrm{Y} \cos^2(\Delta/2) \quad (4)$$

or more conveniently $B(0)/\sin\Delta$ by

$$B(0)/\sin\Delta = (\gamma - 2k) + \delta\mathrm{Y} \cot(\Delta/2) \quad (5)$$

can be obtained from least-squares fitting of the relation between $\Gamma(0, \mathrm{Y}', p, q)$ and Y'.

To obtain γ of the optical system, the specimen is exchanged for some reference crystal which is optically inactive. On the application of the above simple method, $B(0)$ and Δ are measured as a function of an external parameter, temperature T. θ_0, deflecting angles between the principal axis of the indicatrix of the specimen and the observed extinction positions, are also recorded at each temperature. In this case ($k = 0$), the two quantities are simplified to

$$B(0)/\sin\Delta = \gamma + 2\delta\mathrm{Y} \cot(\Delta/2) \quad (6)$$

and

$$\theta_0 = -{}^1/_2(p + q) \cot(\Delta/2) - {}^1/_2\delta\mathrm{Y} \quad (7)$$

When observed values of $B(0)/\sin\Delta$ are plotted against $\cot(\Delta/2)$, γ can be obtained from the intercept of the characteristic line on the ordinate, as can be seen from eq 6. Further, by plotting θ_0 with respect to $\cot(\Delta/2)$, we obtain $p + q$ from the derivative of the characteristic line. Then, it is possible to evaluate p and q separately from these two quantities.

Once p for the optical system has been determined, $B(0)$, $\sin^2(\Delta/2)$ and θ_0 of the specimen are measured as a function of T. $\delta\mathrm{Y}$ can be also measured by the value of $B(0)$ at $2n\pi$, where n is an integer, as can be seen from eq 4. By plotting θ_0 with

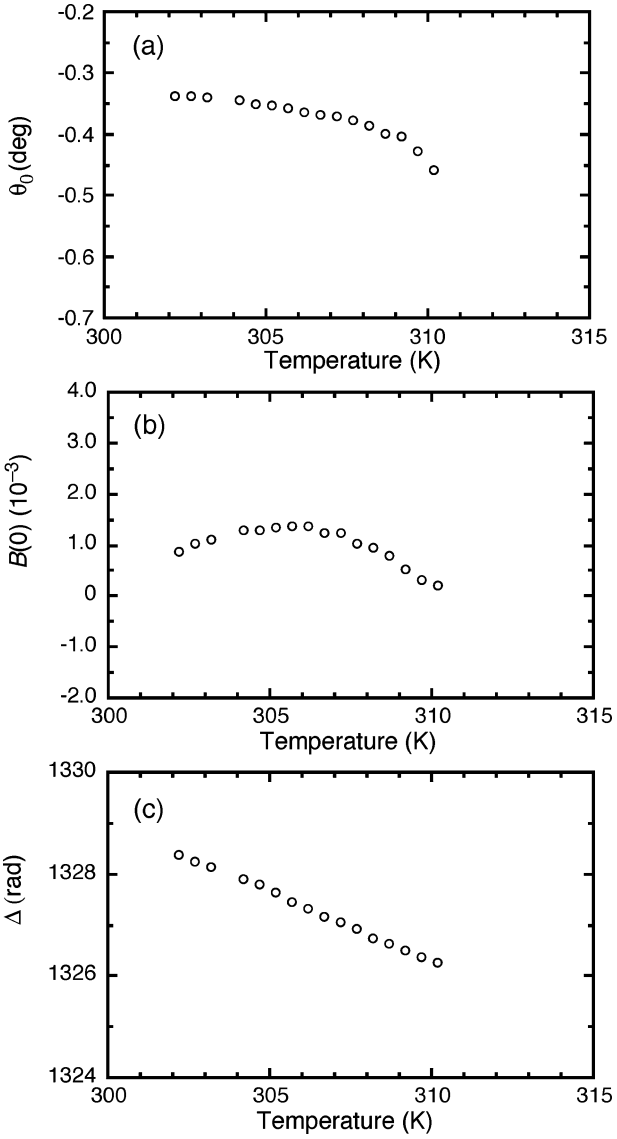

Figure 6. Temperature dependences of (a) Δ_0, (b) $B(0)$, and (c) Δ of (001) plane of *M*-**1·2**.

regard to cot(Δ/2), $p + q$ can be determined from eq 7. Here it must be noticed that θ_0 cannot be measured accurately enough on an absolute scale to evaluate δY, but the relative change with respect to cot(Δ/2) can be measured very accurately. Therefore we can obtain q, and thus finally γ of the optical system. By using these error constants γ and δY, k can be calculated from the relation 5. Then gyration G and birefringence Δn can be determined at each temperature.

We have used the above HAUP method to determine the temperature dependence of all the gyration components and birefringence of both *M*- and *P*-**1·2** using $LiNbO_3$ as a reference crystal. From the symmetry of the crystal, the gyrations G_1, G_2, and G_3 measured on the (100), (010), and (001) planes equal gyration tensor components g_{11}, g_{22}, and g_{33}, respectively. The light source was a He−Ne laser with a wavelength of 632.8 nm. Measurements were performed at around room temperature 300−310 K with an accuracy of ±0.02 K.

First, the (001) specimen of *M*-cocrystal **1·2** was submitted to measurement, because we would like to know to what extent optical activity is induced by the helical structures along the *c* axis (Figures 2 and 3). The temperature dependences of Δ, $B(0)$,

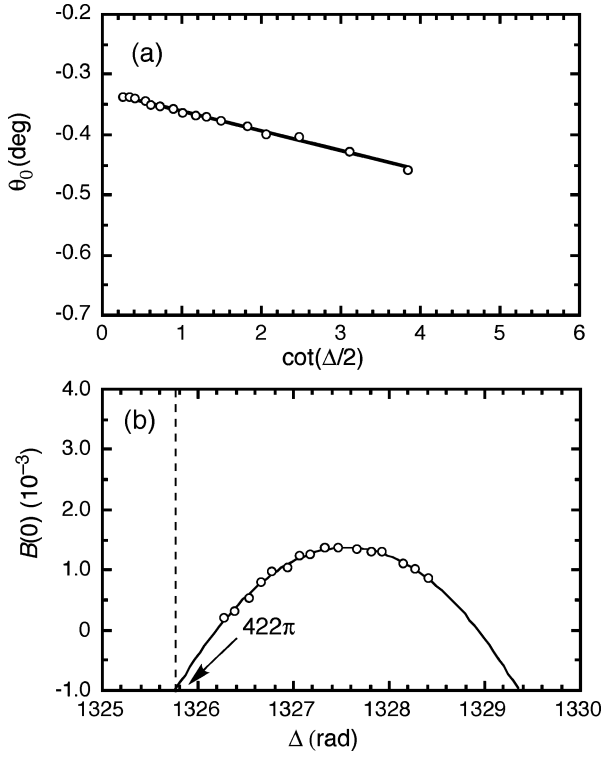

Figure 7. Relation between (a) π_0 and cot(π/2) and between (b) $B(0)$ and π of (001) plane of *M*-**1·2**.

and θ_0 are shown in Figure 6. Then, the relations of θ_0 with cot(Δ/2), and $B(0)$ with Δ were obtained in Figure 7. From the derivative of θ_0 vs cot(Δ/2) (Figure 7a), $p + q$ was determined to be 11.4×10^{-4}. Separately, p was determined to be -1.0×10^{-4} by using an optically inactive $LiNbO_3$ crystal as the standard crystal by the above-mentioned eqs 6 and 7, but the detailed procedure data were omitted here.[4] γ was evaluated to be -1.35×10^{-3}. δY was determined from the value of $B(0)$ at $\Delta = 2 \times 211\pi$ (Figure 7b), where the integer 211 was calculated from the retardation and the negative temperature coefficient measured by using a Berek compensator. The ellipticity k was evaluated from eq 4. Birefringence Δn was calculated from the relationship.

$$\Delta n = (\Delta \times \lambda)/2\pi d \tag{8}$$

where λ expresses the wavelength of the incident light, and d, the thickness of the specimen. The gyration tensor g can be obtained from the relation.

$$g = 2\Delta n \times \bar{n} \times k \tag{9}$$

where $\bar{n}$ represents the mean refractive index. It was determined to be 1.90 by using Chaulnes' method.[27] The temperature dependences of k_3, Δn_c, and g_{33} of the (001) plane of *M*-crystal are depicted in Figure 8.

Next, the (001) plane of the *P*-crystal was submitted to the HAUP measurement. The temperature dependences of k_3, Δn_c, and g_{33} are clarified together in Figure 8, where superscripts M and P designate the *M*- and *P*-crystals, respectively. The gyration tensors g_{33}^{M} and g_{33}^{P} are about -2.4×10^{-3} and $+2.4 \times 10^{-3}$, respectively. The absolute values are coincident each other and

(27) Wahlstrom, E. E. *Optical Crystallography*; John Wiley: New York, 1951; p 66.

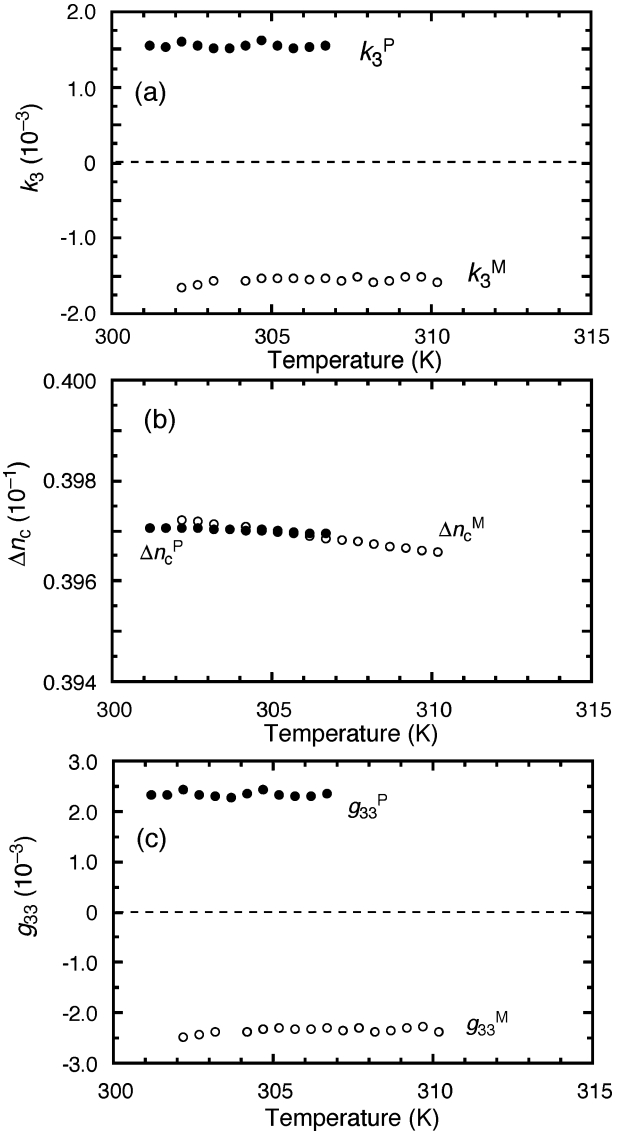

Figure 8. Temperature dependences of (a) k_3 (b) Δn_c, and (c) g_{33} of (001) plane of *M*-**1·2** (○) and *P*-**1·2** (●).

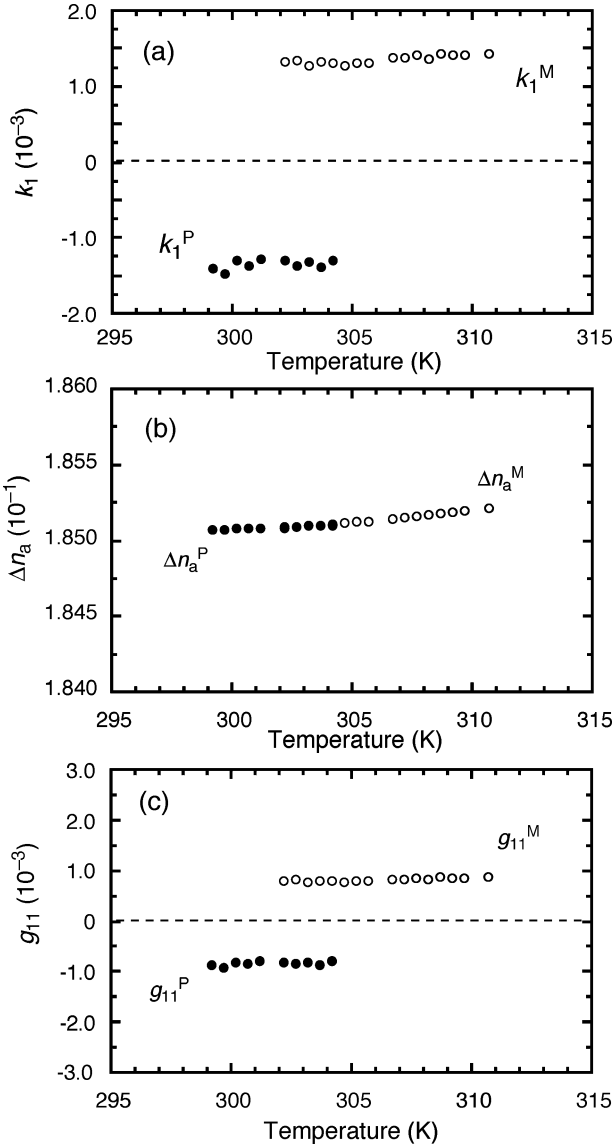

Figure 9. Temperature dependences of (a) k_1 (b) Δn_a, and (c) g_{11} of (100) plane of *M*-**1·2** (○) and *P*-**1·2** (●).

independent of temperature. The birefringences Δn_c^M and Δn_c^P are quite large, 0.397 at 303 K, which is 2.3 times larger than that of calcite ($\Delta n = 0.171$). The birefringences manifest the negative temperature coefficient.

Analogous measurements were performed on the (100) and (010) planes, both of which are perpendicular to each other and to the helical structures along the *c* axis. Figures 9 and 10 depict the temperature dependences of Δ, $B(0)$, and θ_0 of the (100) and (010) planes, respectively, of both of the handed crystals. g_{11}^M and g_{11}^P are about $+0.8 \times 10^{-3}$ and -0.8×10^{-3}, respectively, while g_{22}^M and g_{22}^P are about -0.4×10^{-3} and $+0.4 \times 10^{-3}$, the absolute values being smaller than those of g_{11}^M and g_{11}^P. The magnitudes of Δn_a (0.185) and Δn_b (0.211) are nearly the same as those for calcite, but the temperature coefficients are negative and positive, respectively.

The systematic errors in the present experiments are summarized in Table 1 together with the thicknesses. The order of magnitude of p is 10^{-4}, and those of q, γ, and δY are between 10^{-4} and 10^{-3}. The ellipticities of the cocrystal obtained here are $k_1^M = +1.3 \times 10^{-3}$, $k_1^P = -1.3 \times 10^{-3}$, $k_2^M = -0.5 \times 10^{-3}$, $k_2^P = +0.5 \times 10^{-3}$, $k_3^M = -1.6 \times 10^{-3}$, and $k_3^P = +1.6 \times 10^{-3}$, comparable to the systematic errors. Therefore it is understandable that the consideration of the parasitic ellipticities p and q of the polarizer and analyzer in the HAUP method is inevitable for the determination of the optical activity of the crystal.

Discussion

The gyro-optical properties of *M*- and *P*-**1·2** were successfully determined by the HAUP method at around room temperature for the wavelength 632.8 nm. In chemistry and biochemistry, specific optical rotation $[\alpha]_D$ (degree at 10 cm path length and $c = 1.0$ g per 100 cm^3) has been commonly used as an expression of optical activity in solution. Hence we would like to discuss here the use of optical rotatory power ρ (degree per 1 mm thickness). Optical rotatory power is calculated from the relation

$$\rho = (2 \times 180 \times \Delta n \times k)/\lambda \qquad (10)$$

Figure 11 summarizes the temperature dependences of rotatory powers of both of the handed crystals. The rotatory

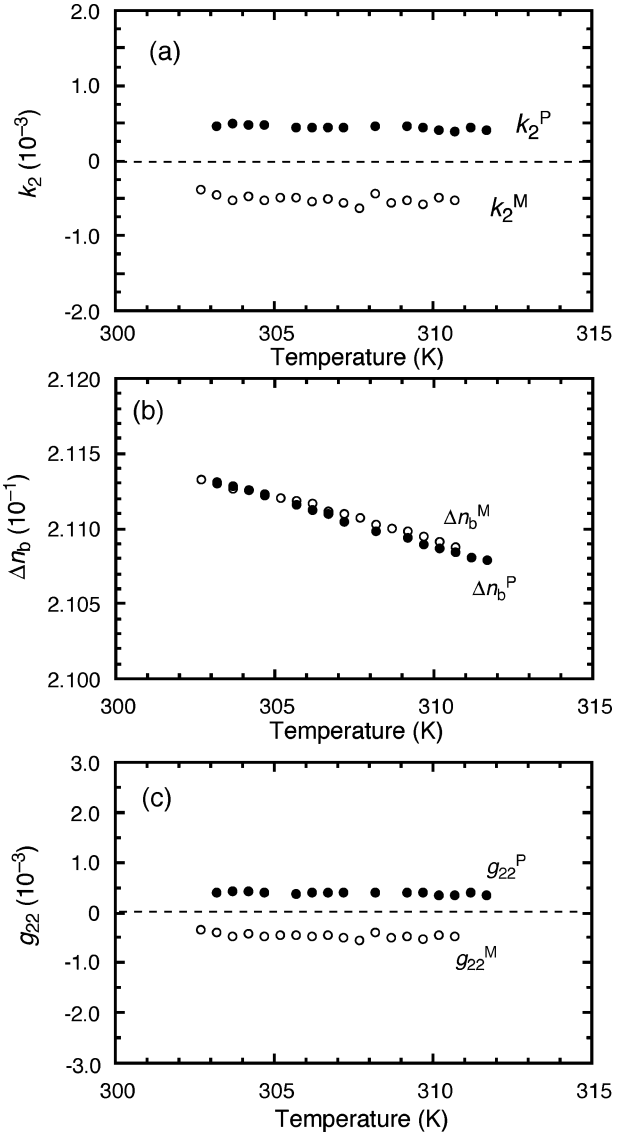

Figure 10. Temperature dependences of (a) k_2 (b) Δn_b, and (c) g_{22} of (010) plane of *M*-**1·2** (○) and *P*-**1·2** (●).

Table 1. Systematic Errors and Thicknesses of Specimens of Cocrystals

		systematic error			
specimen	thickness (μm)	p (10^{-4})	q (10^{-4})	γ (10^{-4})	δY (10^{-4})
M-(100)	461	−3.0	−3.5	0.5	1.7
P-(100)	390	−1.2	13.9	−15.1	−5.9
M-(010)	438	−3.0	8.3	−11.3	−5.5
P-(010)	395	−3.0	−6.4	3.4	0.8
M-(001)	337	−1.0	12.4	−13.5	−3.6
P-(001)	453	−3.0	−4.0	1.0	13.1

powers along the *c* axis of *M*- and *P*-crystal were calculated to be $\rho_3^M = -355$ and $\rho_3^P = +352$ deg mm^{-1} at 303 K (Figure 11c). The absolute values are coincident with each other and almost constant in the present temperature range. The values around −360° and +360° mean that when linear polarized light passes toward us through 1 mm thickness of *M*- and *P*-crystal along the screw axis, the electronic vibration vectors rotate almost one turn in counterclockwise and clockwise directions, respectively. The magnitudes are 10 to 100 times larger than the literature values of the other organic crystals listed in Table 2. Figure 12 illustrates the 2-fold helical arrangements A and

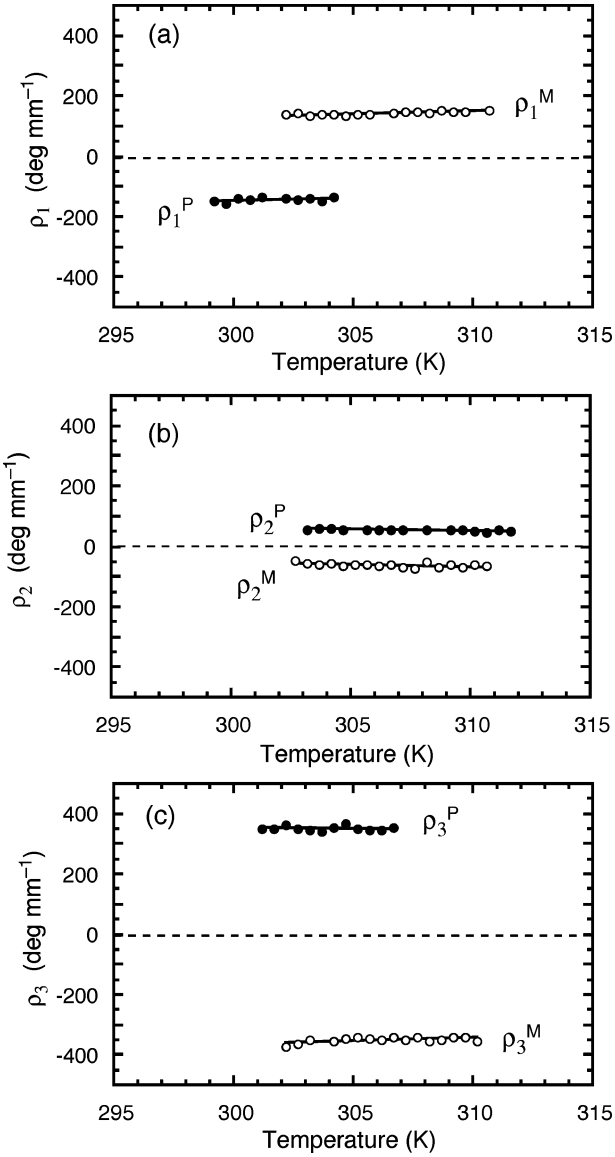

Figure 11. Temperature dependences of (a) ρ_1, (b) ρ_2, and (c) ρ_3 of *M*-**1·2** (○) and *P*-**1·2** (●).

B projected on the (001), (010), and (100) plane. Each length per pitch of the helices A and B is 0.6282 nm, which corresponds to the length of *c* axis of the unit cell. Therefore, the optical rotations of -2.23×10^{-4} and $+2.21 \times 10^{-4}$ degree per pitch are induced by the counterclockwise and clockwise helices A and B in the *M*- and *P*-crystal, respectively.

It is well-known that helicenes are typical molecules having a helical structure. The specific optical rotations $[\alpha]_D$ of [n]-helicenes in solution are huge and increase in proportion to the numbers [n] of aromatic rings.[28−30] For instance, optical rotations of *M*- and *P*-[6]helicene are $[\alpha]_D = -3640$ and +3750, respectively, and those of *M*- and *P*-[10]helicene, −8940 and +8940. Heterohelicenes such as thiahelicenes and oxahelicens are similar.[28,29] Optical activity takes place when the displacement of some electrons is restricted to a helical path under the polarized electromagnetic field. Despite the fact that the $[\alpha]_D$

(28) Laarhoven, W. H.; Prinsen, W. J. C. *Top. Curr. Chem.* **1984**, *125*, 63−130.
(29) Meurer K. P.; Vögtle, F. *Top. Curr. Chem.* **1985**, *125*, 1−76.
(30) Lightner, D. A.; Hefelfinger, D. T.; Powers, T. W.; Frank, G. W.; Trueblood, K. N. *J. Am. Chem. Soc.* **1972**, *94*, 3492−3497.

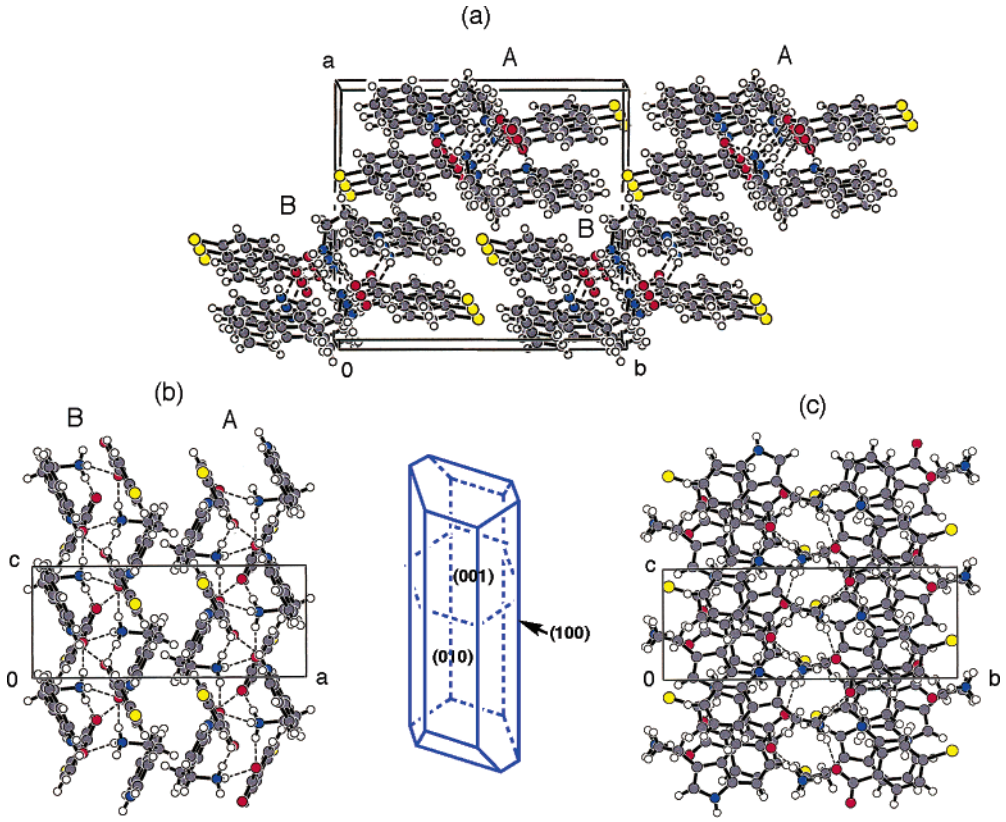

Figure 12. Molecular arrangements on (a) (001), (b) (010), and (c) (100) planes of *M*-**1**·**2**.

Table 2. Optical Rotatory Powers of Organic Crystals

crystal		λ (nm)	T (K)	ρ (deg mm^{-1})	ref
M-tryptamine/ 4-chlorobenzoic acid	ρ_1	632.8	303	+138	this work
	ρ_2			−56	
	ρ_3			−355	
oxo amide	ρ_1	496.5	305	−79	21
	ρ_2			−32	
	ρ_3			−68	
$(NH_2CH_2CO_2H)_3H_2SO_4$		632.8	305	+1.9	16
L-Glutamic acid	ρ_1	632.8	293	−31	17
	ρ_2			−98	
	ρ_3			+5.4	
L-Aspartic acid	ρ_1	632.8	293	+223	18
	ρ_2			−19	
	ρ_3			−31	
Rochelle salt $NaKC_4H_4O_6{\cdot}4H_2O$	ρ_1	632.8	298	−1.0	13
$NaNH_4C_4H_4O_6{\cdot}4H_2O$	ρ_{11}	500	r.t.	3(1)	14
	ρ_{22}			−8(1)	
	ρ_{33}			2(1)	
tartaric acid (2*R*,3*R*)-(+)-$C_4H_6O_6$	ρ_{11}	680	r.t.	+79	15
	ρ_{22}			+90	
	ρ_{33}			−70	
	ρ_{23}			−18	
	ρ			−12.3	
D-mannitol	ρ_1	600	rt	−8(3)	20
	ρ_2			−3.4(3)	
	ρ_3			−57(2)	
lysozyme	ρ_1	488.0	303	−2.1	19
	ρ_3			+2.5	
poly(L-lactide)	ρ_1	514.5	298	+14	12
	ρ_3			+9,200	

values of helicenes in solutions are the mean optical rotations of the whole of helicene molecules measured by the incident light from every direction due to the high mobility in solution, the spiral aromatic π electrons should contribute to the large enhancement of $[\alpha]_\alpha$ values. In our cocrystal **1**·**2**, the phenyl ring of **1** and the indole ring of **2** are arranged in almost parallel manner to form the 2-fold helical structures A and B (Figure 12a,b). Therefore, the helically arranged π electrons along the *c* axis also should enhance the optical rotations, resulting in $\rho_3^M = -355$, $\rho_3^P = +352$ deg mm^{-1}.

Furthermore, there is no doubt that the huge rotatory power ($\rho_3 = +9200$ deg mm^{-1}) of the α-form of the helical polymer film poly(L-lactide) reported by the Kobayashi group[12] is induced by the 10/3 helical molecular chains along the *c* axis (Table 2). In contrast, the rotatory power along the *a* axis, which is in a perpendicular direction to the screw axis, is small ($\rho_1 = +14$ deg mm^{-1}). In the helical structures A and B of our cocrystal **1**·**2**, the 2-fold helical chains are formed through the $NH_3^+\cdots{}^-O_2C$ quaternary ammonium salt bridge and the In−NH···O−C hydrogen bond between the molecules **1** and **2**. The intermolecular helical chains should also contribute to enhancement of the rotations. However, the magnitudes -2.23×10^{-4} and $+2.21 \times 10^{-4}$ degree per pitch in the *M*- and *P*-**1**·**2** are only 1/40 compared with $+7.96 \times 10^{-3}$ degree per pitch in the poly(L-lactide) calculated from the length (2.88 nm) of the *c* axis of the unit cell.

Next, we would like to discuss briefly the sign of rotation obtained here. An *M*-helix (or *P*-helix) is defined as a screw turning in a counterclockwise (or clockwise) direction away from the observer. In contrast, a negative (or positive) sign of rotation is defined as the plane of polarization of light coming toward the observer rotating in counterclockwise (or clockwise) manner. Therefore, the results obtained here seem intuitively to be opposite in that the counterclockwise helical structures of *M*-crystal gave the negative sign of rotation, and the clockwise helices, a plus sign of rotation. In addition, the sign of $[\alpha]_D$ of

M-helicenes in solutions is also always negative, and conversely that of *P*-helicenes is positive.[28−30] It is coincident with our results that the *M*-helix gave the negative rotation ρ_3^M, and the *P*-helix positive rotation ρ_3^P in the crystalline state. The Kobayashi group reported that the positive sign of rotation (+9200 deg mm^{-1}) was induced by the counterclockwise helical molecular chain in the poly(L-lactide) along the *c* axis.[12] However, more recently, Sasaki et al. reported that clockwise and counterclockwise chains coexisted in the α-form of poly(L-lactide) from analysis using the linked-atom least-squares refinements for the X-ray fiber diffraction data.[31] Therefore, the relation between the sign of rotation and the handedness of the helix still remains as an unresolved problem.

The rotatory powers along the *a* axis, which is in a perpendicular direction to the helical structures A and B along the *c* axis, were found to be $\rho_1^M = +138$ and $\rho_1^P = -140$ deg mm^{-1} for *M*- and *P*-**1·2**, respectively. The magnitudes are smaller than those along the screw axis, and the signs are opposite ($\rho_3^M = -355$, $\rho_3^P = +352$ deg mm^{-1}). The aromatic moieties are arranged in an almost parallel manner on the (100) plane (Figure 12c). The incident light along the *a* axis passes the aromatic rings almost perpendicularly.

On the other hand, the rotatory powers along the *b* axis, which is another perpendicular direction to the helices A and B along the *c* axis, were $\rho_2^M = -56$ and $\rho_2^P = +58$ deg mm^{-1} for *M*- and *P*-**1·2**, respectively. As understood from the packing diagram in Figure 12b, the phenyl and the indole moieties are almost perpendicularly arranged to the (010) face in the crystal lattice. Therefore, the incident light along the *b* axis passes the aromatic planes almost parallel to each other. The parallel interaction between the light and the aromatic π electrons might be smaller than the perpendicular interaction on the (100) plane (Figure 12c), to lead to smaller magnitudes than those along the *a* axis ($\rho_1^M = +138$ and $\rho_1^P = -140$ deg mm^{-1}).

The sign and the magnitude of rotatory powers of inorganic crystals could be explained by the anisotropic atomic polarizability theory of optical activity by Grazer and co-workers.[22,23] However, it is impossible to adopt the theory to our organic−organic cocrystal **1·2** because the contribution of not only the molecule itself but also the intermolecular interactions such as the ionic bridge, hydrogen bond, and the $\pi-\pi$ interaction of the aromatic moieties must be considered. Development of theory and computation of optical rotation for organic crystals will be expected in future. In summary, temperature dependences of rotatory powers and birefringence of *M*-crystal are depicted in Figure 13. The quite large birefringences are another feature of the cocrystal together with the large rotatory powers.

(31) Sasaki, S.; Asakura, A. *Macromolecules* **2003**, *36*, 8385−8390.

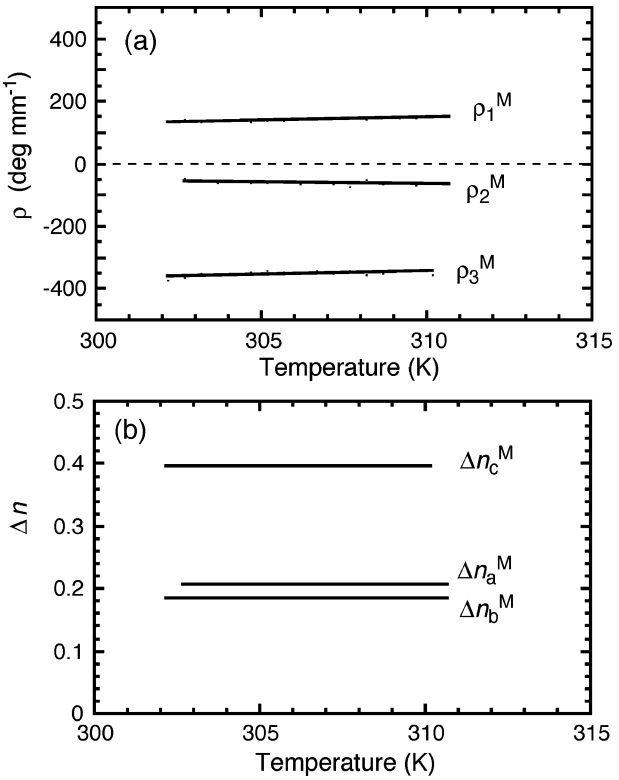

Figure 13. Temperature dependences of (a) optical rotatory powers and (b) birefringences of *M*-**1·2**.

Conclusions

In this study, the optical rotatory powers of the helical-type cocrystal from tryptamine and 4-chlorobenzoic acid were successfully measured by the HAUP method. It was achieved by overcoming the technical problem of the polish of the optical thin specimens. The clockwise helical structures induced the positive sign of rotatory power and the counterclockwise helices negative. The magnitude of the rotatory powers along the helical axis is larger by 1 or 2 orders of magnitude than for ordinary organic crystals. The large rotatory powers are induced by the intermolecular helical structures formed between the two components through the ionic bridge, the hydrogen bond, and the aromatic $\pi-\pi$ interaction.

Acknowledgment. This paper is dedicated to Emeritus Professor Teruo Matsuura who died in May 2004. This research was supported by a Grant-in-Aid for Scientific Research from the Ministry of Education, Sports, Culture, Science and Technology (MEXT), Japan.

Supporting Information Available: X-ray crystallograhic data (CIF) of cocrystal *P*-**1·2**. This material is available free of charge via the Internet at http://pubs.acs.org.

JA044472F